The Impact of Matrix Heterogeneity on Gamma-Ray Waste Assay

Brian M. Young, Stephen Croft, and Robert D. McElroy
Canberra Industries, Inc., 800 Research Parkway, Meriden CT 06450, USA.

Abstract
The quantification of gamma emitting radionuclides in large waste packages has traditionally been based on segment response functions for homogeneous matrices with uniform activity distributions. This is usually justified on the grounds that in the absence of additional information, the assumption of uniformity would, on the average when taken over a large number of containers, approximate the situation for randomly packed waste. The stream average (or cumulative) assay result would therefore presumably not be biased. In practice, however, the matrix in a particular container may be quite heterogeneous, consisting of chunks of material with void space between. Additionally, the activity distribution may not match the density distribution of the matrix. An example is surface contamination chunks of material in a heterogeneous container. The impact of these deviations from the simplistic assumptions of matrix and source uniformity have not been extensively studied and reported previously.

In this work we look at the problem using a numerical simulation tool especially constructed to model irregular density and activity distributions. We illustrate for two familiar assay conditions - the gamma-ray assay of 200 liter drums and SLB-2 waste boxes - how the presence of substantial void space results in a higher detection efficiency than the usually applied uniform model would predict. We show how with reasonable knowledge of the waste form, an allowance may be made and in particular how a more appropriate total measurement uncertainty (TMU) contribution may be estimated.

Introduction
The need for non-destructive radioassay of potentially active or contaminated material in containers such as the familiar 200 liter drum and larger B-25 boxes is common place. Within the U.S. Department of Energy community, the Standard Large Box 2 (SLB2, approx. 7000 liters) and the Standard Waste Box (SWB, approx 2000 liters) also find frequent use. For purposes of screening and free release, two competing objectives in the design of any gamma-ray assay system are: high throughput and high sensitivity. A typical strategy for meeting both measurement objectives within the known constraints of the problem is to assay the container from many detector positions so as to ensure that the entire sample volume is “seen” by at least one detector. Typically multiple detectors acquire data concurrently.

An example implementation of such an approach is the Canberra WM-2500 Series Box Counter. In this system, four high-purity germanium (HPGe) detectors are used to assay the item. Two detectors are stacked vertically on either side of the container, which moves on a trolley between the two detector assemblies. The assay takes place with the trolley and sample located at multiple stationary positions along its length. So, if a large box such as an SLB2 is assayed, for example, with five trolley positions, and with four detectors counting at each position, there are thus a total of 20 detector locations which comprise the assay dataset. This is depicted in Figure 1.

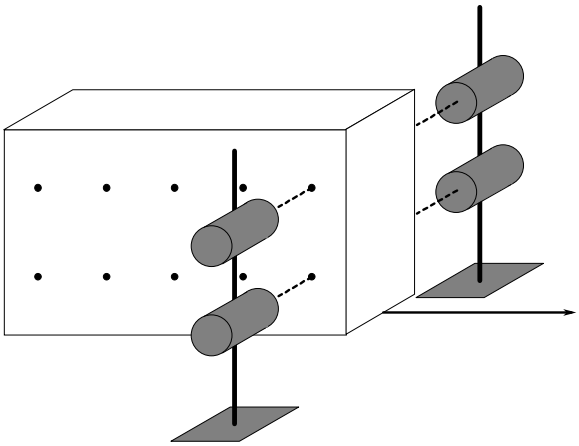

Figure 1. Illustration of a typical Box Counter measurement geometry.

For multi-position assays such as this, the most sensitive measurement result, that is the one with the lowest detection limit, is generally obtained from analyzing the summed spectrum from all of the detector locations. In order to obtain activity values from the accumulated spectrum, an efficiency calibration (i.e. full-energy-peak counts registered in the spectrum per gamma-ray emitted in the sample medium) must be used. Typically the efficiency used during data analysis is obtained assuming that both the activity and the attenuating sample matrix are uniformly distributed throughout the volume of the container. Uniformity is very rarely realized with actual sample waste containers. There are several reasons for nevertheless making the assumption of uniformity. For one it simplifies calibration – whether one calibrates via measurement of prepared surrogates or via mathematical calculations, it is often cheaper, faster, and easier to use a uniform source term. Another, more important, reason is that if a large number of containers is to be counted, each with its own unknown degree and configuration of nonuniformity, the only reasonable assumption one *can* make is that of uniformity. It is requires no prior information about the item. It does assume random packing and filling for each individual container; but such an assumption is frequently justified. However, for a given container the difference between the actual (and usually unknown) source and matrix configuration and the uniformity that is assumed in the efficiency calibration can have significant impact on the accuracy of the final assay result.

The origin of these effects can easily be understood by examining a general expression for the summed efficiency for several detectors counting a container volume with arbitrary distributions of activity and attenuating matrix.

$$\varepsilon = \frac{1}{A_{Total}} \sum_{\text{Detectors}} \int_{\text{Container}} A(\vec{r}) \cdot \frac{e^{-\mu(\vec{r}) \cdot x(\vec{r})}}{d(\vec{r})^2} \cdot F(\theta_{\vec{r}}) \cdot dV$$

In this expression, each differential volume unit dV has an activity concentration A. A line of sight exists between the point source $A.dV$ and each detector. This vector has a total length d, and passes through attenuating materials described by the linear attenuation coefficient μ over the path-length x on its way out of the container. The function F represents the angular response of each detector for off-axis rays. Nearly every quantity in the integrand is labeled with the notation $\vec{r}$ to emphasize its dependence on position within the container volume. Nonuniformities enter the calculation explicitly in two places – the activity distribution within the sample volume is

represented by the quantity $A(\vec{r})$, and the distribution of attenuating matrix is represented by the combined quantity $\mu(\vec{r}) \cdot x(\vec{r})$. The quantities $\mu(\vec{r})$ and (but often to a lesser degree) $F(\theta_{\vec{r}})$ are both also energy dependent. The uniform case results when both $A(\vec{r})$ and $\mu(\vec{r})$ are constant, independent of position.

For any given, generally nonuniform, container, the efficiency can be represented by the quantity $\varepsilon_{\text{Nonuniform}}$. The uniform efficiency, assumed for calibration, can be represented by the quantity $\varepsilon_{\text{Unif., Calib.}}$. Thus, when the container is assayed, the ratio of the measured activity to the true activity is given by the ratio $R = \frac{\varepsilon_{\text{Nonuniform}}}{\varepsilon_{\text{Unif., Calib.}}}$. If the sample item is indeed homogeneous in matrix and uniform in activity – in other words if the sample geometry matches the calibration geometry – then the ratio is unity. It is also easy to see that substantial discrepancies can also arise. For instance, if the activity exists as a single concentration buried deep in the container, then few (or no) gamma-rays may survive unattenuated to the detectors, and the measured activity will be lower than the true activity. Alternatively, if the activity is concentrated on the periphery of the container, shining brightly into the detectors, then the measured activity will be higher than the true activity. One can quantify these extreme limits rather simply by hand calculations or via physics software such as MCNP^{TM} [1] or Canberra's ISOCS [2]. However, this approach usually requires individual calculation of each nonuniform geometry and has thus primarily been used to examine the extreme or bounding cases. More generally one would like to examine the probability distribution of ratios for a large population of nonuniform cases. From this distribution it is possible to examine such quantities as the population average, the most likely ratio, and confidence intervals.

Monte Carlo Technique

To facilitate this sort of examination, a dedicated Monte Carlo technique has been developed to explore the distribution of *R* values for point activities randomly distributed inside randomly-configured sample matrices. The details of this technique have been presented elsewhere [3], and a brief outline is given here.

The efficiency equation given above is evaluated for the sum of detectors in a computer code for a series of randomly-placed point sources inside a randomly configured container. The primary input required by the code consists of the dimensions of the container, the locations of the gamma-ray detectors (assumed to be pointlike since there are small compared to the general dimensions of the problem and it is only the relative matrix behavior that we are concerned with), and the number of point sources assumed to be randomly positioned within the container volume. Attenuating materials in the sample matrix are specified by attenuation coefficient values μ expressed in units of cm^{-1}. Note that this encompasses three physical aspects of the measurement problem – the photon energy, the attenuating material, and the density of the material. Nonuniform matrices are treated by specifying a series of attenuation coefficients and volume fractions for the various materials that make up the overall sample. In the Monte Carlo model, the sample matrix is assumed to be divided into a 20 x 20 x 20 three-dimensional grid of volume elements (i.e. "voxels"). To set up a single random case, the 8000 voxels are randomly populated with attenuation coefficient values with the appropriate volume fractions (i.e. probabilities) from the information described above.

To evaluate the efficiency for a single random configuration, the source points are randomly placed and matrix voxels are randomly populated, and the efficiency is calculated using the following discrete expression which is explicitly analogous to the equation presented above in the Introduction. The physical model is depicted in Figure 2.

$$\varepsilon_{\text{Nonuniform}} = \frac{1}{\sum_{\text{Pt Src } i}^{N} A_i} \cdot \left(\sum_{\text{Pt Src } i}^{N} \sum_{\text{Pt Det } j} A_i \cdot \frac{e^{-\sum_{\text{Path } k(i,j)} \mu_k x_k}}{d_{ij}^2} \cdot F(\theta_{ij}) \right)$$

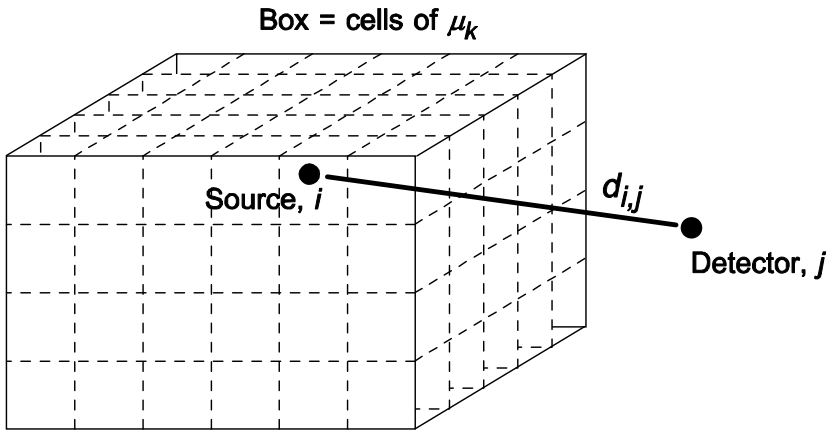

Figure 2. Illustration of the model implemented in the Monte Carlo software.

From the material specifications, the volume-average attenuation coefficient is calculated. This is used to populate a uniform matrix and the above expression is evaluated for "many" (typically 10^6-10^7) random point source locations. In effect, this evaluates the uniform volume integral. The assay ratio *R* for a given nonuniform case is then the ratio of the calculated efficiencies for the nonuniform and the uniform case.

Results for Large Boxes – SLB2 Containers

Calculations were run for SLB2, boxes roughly 165 cm x 165 cm x 265 cm with steel walls roughly 0.4 cm thick. Calculations were run for all combinations (182 in total) of the seven energies and 26 material-density-void fraction combinations listed in Table 1.

Energy (keV)		Material, Density ($g \cdot cm^{-3}$)	Void Fractions (%)
59	(^{241}Am)	Air, 0.0012	0 (Air *is* void)
129	(^{239}Pu)	Cellulose, 0.1	0, 10, 20, 30
186	(^{235}U)	Cellulose, 0.4	0, 10, 20, 30
414	(^{239}Pu)	Concrete, 0.7	0, 10, 20, 30, 40
662	(^{137}Cs)	Concrete, 1.0	0, 10, 20, 30, 40
1001	(^{238}U)	Concrete/Steel, 1.6	0, 10, 20, 30, 40, 60, 80
1333	(^{60}Co)		

Table 1. Summary of lines and materials modeled.

For a given material-density combination, the bulk density was held constant for various void fractions. This was done by scaling the density of each material appropriately. For example, consider the "Concrete, 1.0 g·cm^{-3}" combination. For a void fraction of 0%, the matrix was completely filled with concrete at 1.0 g·cm^{-3}. For a void fraction of 20%, one fifth of the matrix voxels were filled with air (density roughly 0 g·cm^{-3}), and four fifths of the voxels were filled with concrete at a density of 1.25 g·cm^{-3}. Thus the bulk density of the matrix (0.2 * 0 g·cm^{-3} + 0.8 * 1.25 g·cm^{-3}) remained unchanged.

For each combination (i.e. for each μ value and void fraction), 500,000 configurations were run assuming five point sources randomly placed within the container volume. The counting geometry was typical for a Canberra WM-2500 Series Box Counter – 20 detector positions (i.e. four detectors at five trolley positions along the length of the box) at a distance of roughly 60 cm from the sides of the box. The overall behavior of the ratio distributions versus sample bulk density has been presented in detail in earlier work [3] for uniform matrices. This behavior versus bulk density is still present with nonuniform matrices. The emphasis here is on the behavior versus void fraction. As an example, the frequency (probability) distributions of the assay ratios are presented in Figure 3 below for a representative material-density combination at 662 keV, for five values of void fraction.

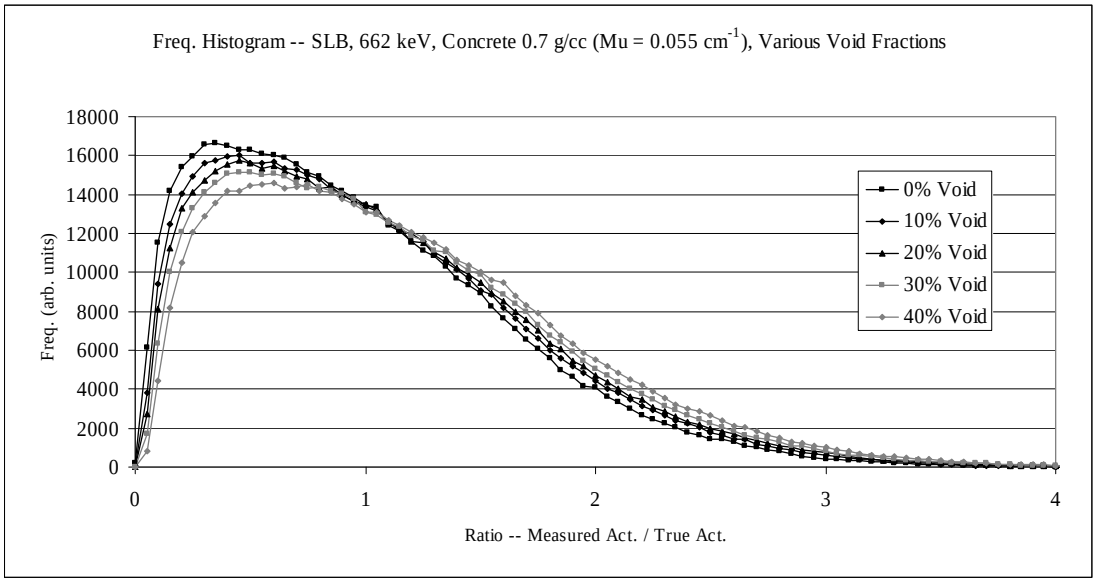

Figure 3. Frequency distribution of measured to true activity at 662 keV for the case of the SLB2 simulations.

The obvious feature here is that higher void fractions tend to shift the probability distribution towards higher ratios – the low-ratio end of the distribution assumes a smaller slope and the high-ratio end of the distribution is extended. As discussed elsewhere [3], for the case of a uniform matrix (0% void fraction), the distribution is determined solely from the random placement of sources in the matrix, and the average ratio is unity. However, this is not the case when void space is present. The average ratio increases with increasing void space. This is depicted in Figure 4 below, which shows the average ratio values versus μ value and void fraction. For uniform matrices, the mean values all like along the unit line. For higher void

fractions and higher μ values, the ratios increase markedly. This increase in ratio is evidently due to the increasing likelihood of shine paths from the source point to one or more detectors.

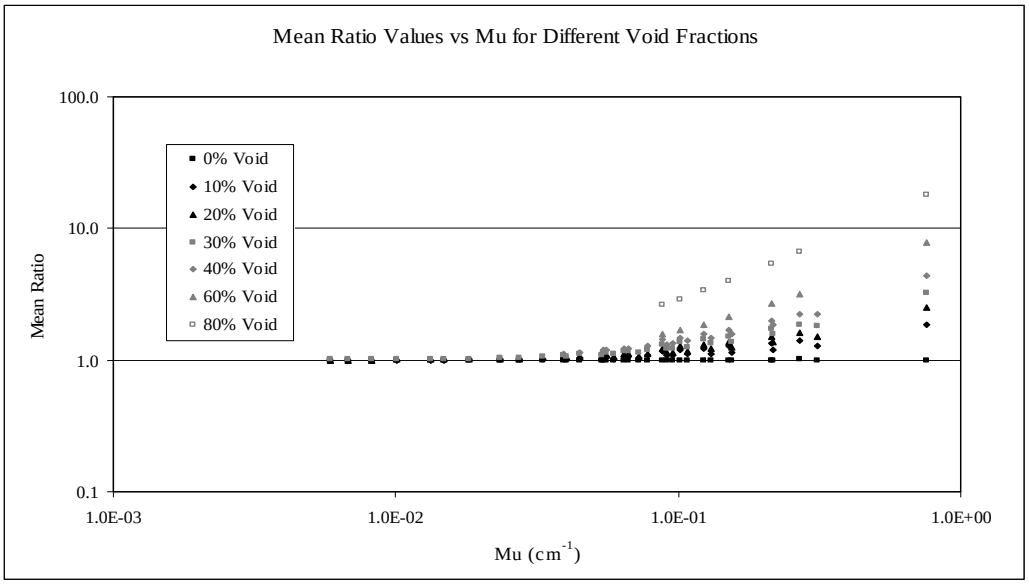

Figure 4. Mean ratio values for the SLB2.

It should be noted that most common assay situations dealing with containers as large as an SLB2 are restricted to attenuation coefficient values (i.e. energy-material-bulk density) ranging from 0.01 to 0.1 cm^{-1}, and void fractions typically no more than 40%. Within this range, the estimated mean ratio (i.e. bias) is no more than roughly a 1.3 (i.e. a 30% overestimate of the true activity in the container) for the highest attenuations.

One can also estimate confidence bands from these distributions [3]. A common starting point for estimating total measurement uncertainty (TMU) values is to create $\pm 3\sigma$ bounds (where σ denotes the standard deviation). These bounds are presented in Figures 5 and 6 below.

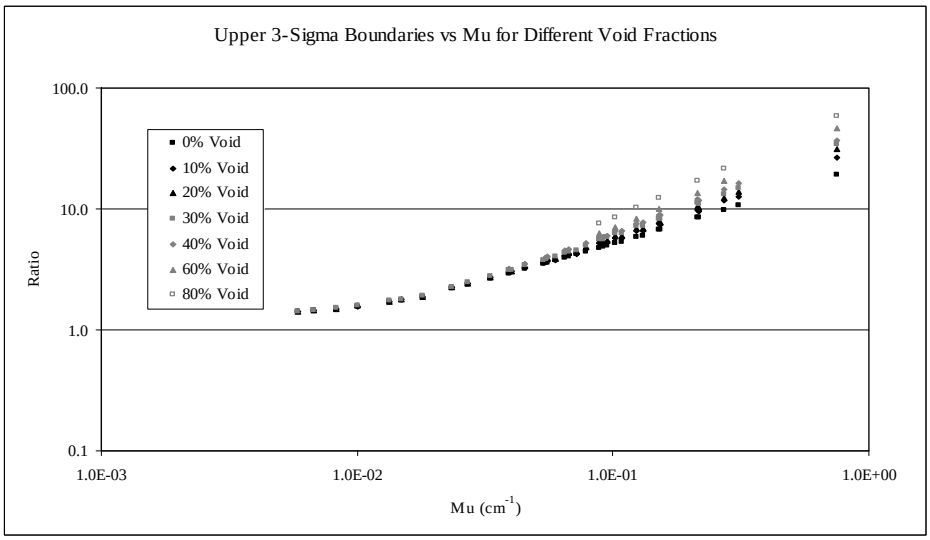

Figure 5. Upper 3σ bounds for the SLB2.

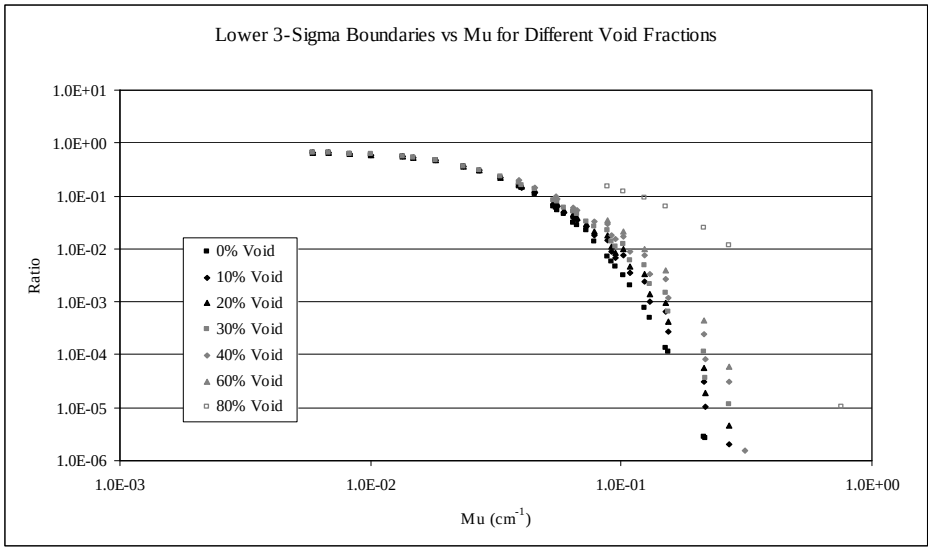

Figure 6. Lower 3σ bounds for the SLB2.

As expected [3], the bounds deviate further from unity with increasing attenuation. Note, however, that *both* the upper and lower bounds also increase with void fraction, as is consistent with the entire assay probability distribution shifting upwards with increasing void fraction. The conservative approach in estimating the TMU boundaries would be to take the "worst case" position in either direction. Assuming typical assay conditions as above, attenuation coefficient values ranging from 0.01 to 0.1 cm^{-1}, and void fractions typically no more than 40%, the upper bound would correspond to roughly a factor of 8 overestimate (40% void fraction) and the lower bound would correspond to roughly a factor of 300 underestimate (uniform matrix case) for the highest attenuations.

Results for 200 Liter Drums

A similar campaign of calculations was run for rotating 200 liter drums. For each combination (i.e. for each μ value and void fraction), 500,000 configurations were run assuming three point sources randomly placed within the drum (three points rather than five is a concession to reduced drum volume). As above, the counting geometry was typical for a WM-2500 Series Box Counter, with four detector positions (i.e. only one trolley position, centering the detectors on the drum axis) at a distance of roughly 60 cm from the sides of the drum. The frequency distributions show similar features to the ones presented above for the SLB2. Naturally, since the 200 liter drum is a smaller container, the distributions are not as drastically skewed as the ones above, but they still shift towards higher ratios with increasing void fraction. Presented in Figure 7 below are the average ratio values versus μ value and void fraction. The behavior is very similar to that for the SLB2, but the deviations from unity aren't as extreme, due to the smaller size of the container and hence weaker overall attenuation for a given matrix type. When restricted to typical linear attenuation values between 0.01 and 0.1 cm^{-1} and void fractions below 40%, the worst mean ratio bias is no more than roughly 1.1 for the most attenuating cases.

The 3σ bounds (not plotted) also behave similarly to those for the SLB2; and as expected, the deviations aren't as extreme. At the typical assay conditions assumed above, the bounds correspond to roughly factors of 3 to 5 in both directions.

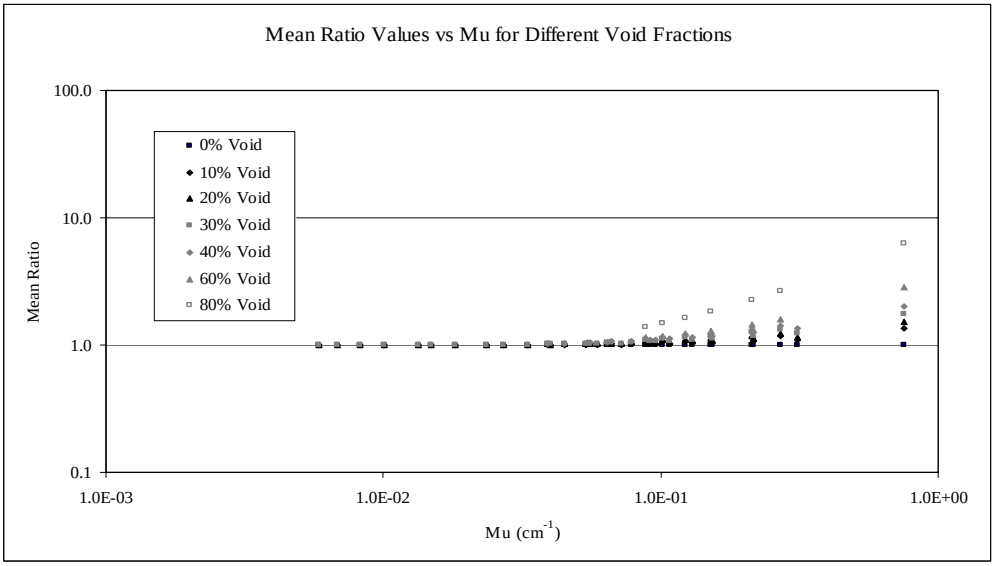

Figure 7. Mean ratio values for the 200 liter drum.

Discussion and Conclusions

The bespoke Monte Carlo tool introduced in [3] has been used to explore the effects of void space on the results of gamma-ray assays of large containers. The overall features and behavior of the distributions of assay results versus matrix attenuation (i.e. bulk average μ value) are very similar to those reported earlier. The addition of void space in the matrices, however, adds a bias to the distributions – assays of containers with void space will tend to overestimate the true activity when a uniform calibration is used. In truth, this bias (tens of percent in the cases examined here) are quite small compared with the 3σ TMU estimates (which are factors of several in the over reporting direction and factors of "hundreds" in the under reporting direction, for the present cases studied) which are dominated by the source nonuniformity. It may be feasible for some applications to consider these biases negligible as compared to the TMU's especially if some effort is made at the time of physical calibration to incorporate some non-homogeneity into the items being used. On the other hand, all of the curves presented appear to be well behaved, which implies a rough parameterization is possible. One could use prior knowledge, RTR images, etc. to estimate the void fraction in a given container and use that in addition to knowledge about the bulk matrix density to correct for this bias and also obtain improved TMU estimates.

References

[1] X-5 Monte Carlo Team, "MCNP – A General Monte Carlo N-Particle Transport Code, Version 5", LANL Publications LA-UR-03-1987, LA-CP-03-0245, and LA-CP-03-0284.

[2] R. Venkataraman, F. Bronson, V. Atrashkevich, B. M. Young, and M. field, "Validation of in situ object counting system (ISOCS) mathematical efficiency calibration software", *Nuclear Instruments and Methods in Physics Research*, A442 (1999) 450.

[3] B. M. Young, S. Croft, and H. Zhu, "The Influence of Source and Matrix Nonuniformity on the TMU and Bias of Large Container Gamma-Ray Assay Results", *Proceedings of 47th INMM Annual Meeting, 2006, Nashville, TN.*